W and Z Measurements with Initial CMS Data

David Wardrope
Imperial College London
On Behalf of the CMS Collaboration

Abstract

The CMS analysis strategy for the early data measurement of the inclusive W and Z production cross-sections using their electron and muon decay modes, with an integrated luminosity of $10\,\mathrm{pb}^{-1}$, is outlined. This measurement is expected to be among the first from the LHC and so focus is placed on the use of robust selections and data-driven methods to cope with the effects of the detector misalignment and miscalibration expected shortly after start-up. Preliminary results, obtained using data from a detector fully simulated with the expected imperfections, are presented.

1 Introduction

There are several compelling reasons for measuring the inclusive W and Z production cross-sections using their decay modes to electrons [1] and muons [2] in the early data from CMS. The production of W and Z bosons is well understood theoretically [3] and has been experimentally tested to great precision [4] since their discovery in the early 1980s. The principal theoretical uncertainties that concern their production at the LHC are from radiative corrections and those arising from uncertainties on the parton density functions of the proton.

The high centre of mass energy at the LHC will allow measurements in new, unprobed energy regime. 'Rediscovering' the physics of the electroweak sector is a vital activity in order to understand both the physics of the LHC and the use of the CMS detector to reconstruct it. Precise measurements, together with good theoretical understanding, of W and Z production can constrain parton density functions, as these processes are sensitive to the internal structure of the proton. Furthermore, making cross-section measurements requires a good knowledge of trigger, reconstruction and selection efficiencies, useful for a wide range of analyses.

W and Z bosons are predicted to have large production cross-sections at the LHC, approximately 190 nb and 60 nb respectively [3]. Their experimental signature of well-isolated leptons with high transverse momenta is very distinctive in hadron collisions and should be readily triggered and selected. Thus, an integrated luminosity of only $10\,\mathrm{pb}^{-1}$ is sufficient for significant analyses of W and Z production.

An inclusive cross-section measurement made with $10\,\mathrm{pb}^{-1}$ will be one of the first results from CMS and the LHC. For this early data, the ultimate calibration and alignment of the detector will not be available and so the analyses described here place emphasis on mitigating any effects consequent to this : simple and robust selections and data-driven methods are used to measure efficiencies and estimate signal and background yields in order to reduce sensitivity to the Monte Carlo modelling of CMS and the LHC environment.

The focus of the analyses was on developing and testing these methods as realistically as possible. To this end, the data used was from a detector simulated with miscalibrations and misalignments on the level we expect shortly after start-up.

2 Reconstruction and Selection of W and Z Bosons

The design of the CMS detector [5] is based around a 4 T large radius solenoid, containing the silicon-based inner tracking; the homogeneous, fully active, crystal electromagnetic calorimeter (ECAL); and the sampling hadronic calorimeter (HCAL). Outside the solenoid are four layers of muon detectors, installed in

the solenoid return yoke.

2.1 Decays to Electrons

$W \to e\nu$ and $\gamma^*/Z \to ee$ events must pass the single isolated electron High Level Trigger requirements [6]. Further offline selection of $W \to e\nu$ requires one offline reconstructed electron within these events and $\gamma^*/Z \to ee$ requires two. An offline reconstructed electron [5] consists of a supercluster in the ECAL, matched to a track from the interaction vertex. The supercluster is a collection of clusters, extended in the azimuthal direction to gather the energy radiated by an electron traversing the tracker.

The reconstructed electrons in both event types must satisfy some robust identification criteria based on cluster shape and track-supercluster matching, which are designed to be efficient and effective at start-up when CMS is not calibrated or aligned to the ultimate precision. In order to select the high p_T, isolated electrons characteristic of W and Z decay, the electrons' superclusters must be within the fiducial volume of the ECAL ($|\eta|$ <1.44 and 1.56< $|\eta|$ <2.5), with transverse energy > 20 GeV. Low charged particle activity around the electron is demanded in the tracker.

In $W \to l\nu$ events, the presence of the neutrino is inferred by an imbalance in the transverse energy vector sum of the event, $\not{E}_T$. This missing transverse energy, calculated from calorimeter energy deposits, is used as a further discriminating variable for the estimation of signal and background event yields.

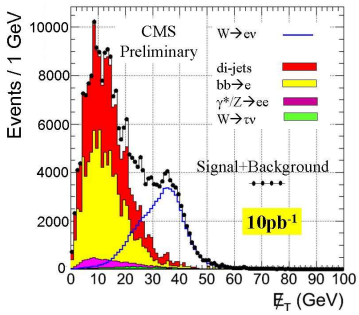

Figure 1: $\not{E}_T$

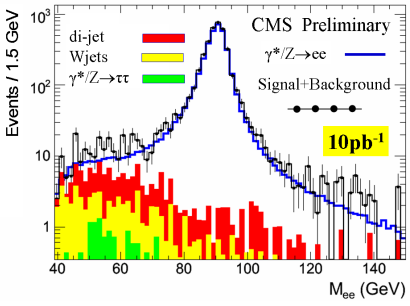

Figure 2: *Invariant*

2.2 Decays to Muons

$W \to \mu\nu$ and $\gamma^*/Z \to \mu\mu$ events are first triggered by the single muon trigger [6]. Offline, muons are reconstructed by both the inner tracking detector and the dedicated muon chambers outside the solenoid. A global muon has its trajectory reconstructed using hits in both of these subdetectors. All muons are required to have low charged particle track activity around them.

The selection of $W \to \mu\nu$ events requires the presence of an isolated global muon with $p_T > 25\,\text{GeV}$, with $|\eta| < 2$. The transverse mass, m_T, of the W is formed, interpreting the $\not{E}_T$ as the neutrino's p_T. $m_T > 50\,\text{GeV}$ is required.

$$m_T = \sqrt{2p_T^l p_T^\nu \left(1 - \cos\left(p_T^l, p_T^\nu\right)\right)} \tag{1}$$

$\gamma^*/Z \to \mu\mu$ events are selected by requiring two muons, at least one of which must be global. The other muon may be global or – in order to increase selection efficiency – may be reconstructed either in the muon chambers or inner tracker alone. Both muons must have $p_T > 20\,\text{GeV}$ and be within the muon system fiducial volume ($|\eta|$ <2.5). The invariant mass of the muon pair is required to be above 40 GeV.

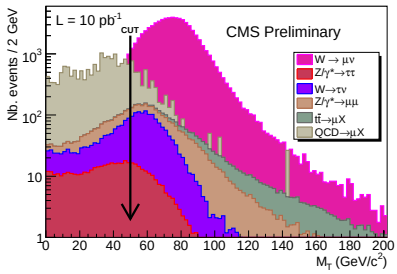

Figure 3: *m_T distribution of $W \to \mu\nu$ and its backgrounds, after selection. The number of events used correspond to those expected for $10\,pb^{-1}$ of integrated luminosity. The cut at m_T = 50 GeV is indicated.*

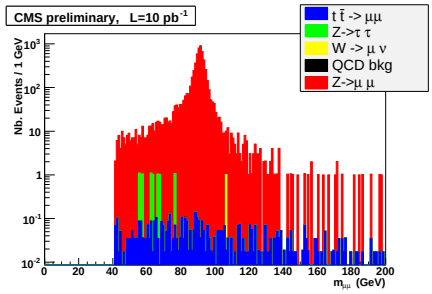

Figure 4: *Invariant mass distribution of $\gamma^*/Z \to \mu\mu$ and its backgrounds, after selection of events with two global muons. The number of events used correspond to those expected for $10\,pb^{-1}$ of integrated luminosity.*

3 Efficiency Determination from Data

The efficiency to reconstruct objects and to trigger and select events can be measured using the data-driven "Tag and Probe" method [7]. An unbiased and pure sample of leptons is obtained from $Z \to ll$ for measuring the efficiency of a particular cut, trigger threshold or reconstruction step. One lepton, the "tag", meets stringent identification criteria. The other, "probe", lepton need satisfy only loose criteria that are appropriate to the efficiency under study and leaves it unbiased with respect to it. The purity of the probe sample is ensured by restricting the invariant mass of the lepton pair to be about the Z mass pole.

The efficiencies measured using the Tag and Probe method have been validated against the true efficiencies from Monte Carlo simulations. An example of the good level of agreement found is shown in Figure 5.

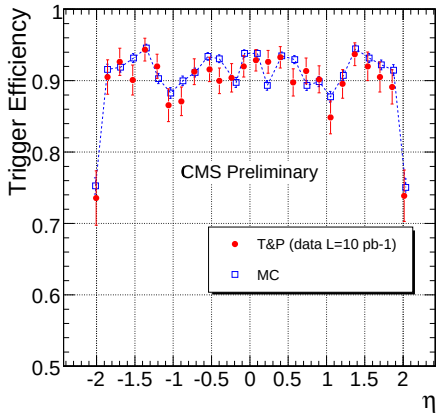

Figure 5: *Efficiency as a function of the pseudorapidity, η, for a global muon with $p_T > 20$ GeV in selected $Z \to \mu\mu$ events to satisfy the single muon trigger criteria. A good level of agreement is observed between the true efficiency (open squares) and the efficiency determined using Tag and Probe (filled circles) with data corresponding to 10 pb^{-1} of integrated luminosity. Statistical uncertainties are shown for the Tag and Probe efficiencies.*

4 Background Estimation

Electroweak backgrounds in the W and Z samples are small and sufficiently well understood theoretically, so they can be reliably estimated from simulation.

However, the QCD backgrounds are much larger and more difficult to simulate, particularly in the case of $W \to e\nu$. As a result several data-driven background subtraction methods have been evaluated for use on data.

The template method uses predefined distributions of some background discriminating variable, "templates". Separate templates for selected signal and background events are determined and are simultaneously fit to the distribution of the selected sample (which contains both signal and background). The templates have free normalisation and so the number of both signal and background events can be estimated. Both signal and background templates can be determined from data.

The templates for $W \to l\nu$ are determined from data using $Z \to ll$ events. In the muon case, the missing transverse energy distribution and the transverse energy direction resolution observed in $Z \to \mu\mu$ are parameterised appropriately in terms of the Z momentum. These are then interpreted as predictions for the $W \to \mu\nu$ $\not\!\!E_T$, and can be combined to form a m_T template, Figure 6. The transverse energy magnitude and its direction are considered uncorrelated.

In the $W \to e\nu$ channel, the template for the dominant QCD di-jet background can be determined by making the selection, but inverting the track isolation criterion. This has the effect of anti-selecting the signal and also the electroweak backgrounds, leaving a pure di-jet sample. The $\not\!\!E_T$distribution of this sample seems to be a good template for the isolated background (Figure 7), as the isolation condition applied to the jets and $\not\!\!E_T$are largely uncorrelated.

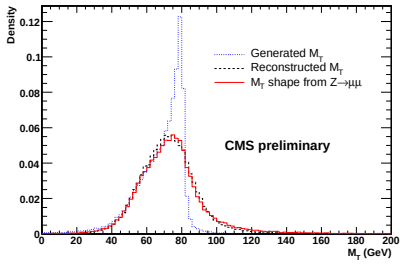

Figure 6: *The m_T distribution of the selected $W \to e\nu$ sample (dashed line) is well represented by the template derived from $Z \to \mu\mu$ events (solid line).*

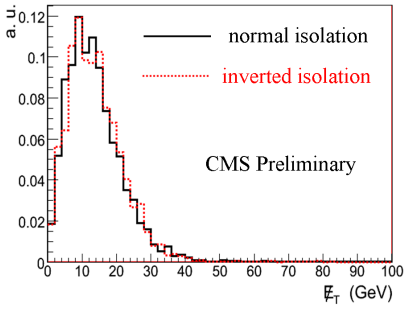

Figure 7: *The $\not\!\!E_T$ distribution of QCD di-jet events passing the selection (solid line) is well represented by the template derived from the inverted isolation sample (dashed line).*

5 Cross-section Measurement

The W $\rightarrow$ lν cross section is calculated using the following formula (similarly for γ^*/Z $\rightarrow$ ll):

$$\sigma_W \times BR(W \rightarrow l\nu) = \frac{N_W^{sig} - N_W^{bkgd}}{A_W \times \epsilon_W \times \int Ldt} \quad (2)$$

N_W^{sig} and N_W^{bkgd} are the number of signal and background events passing the selection. ϵ_W is the efficiency of the triggering, reconstruction and selection of the $W \rightarrow l\nu$ events. All are measured from data using the methods described. A_W is the geometric and kinematic acceptance of $W \rightarrow l\nu$ events, which is determined from simulation. The integrated luminosity, $\int Ldt$, is measured externally to these analyses.

The results of the calculations for W $\rightarrow$ eν are shown in Table 1. There is good agreement between the data-driven cross-section determination and the cross-section input to the analysis. It should be noted that the uncertainties in the table are purely statistical and a systematic uncertainty of $\sim$10% is anticipated on the integrated luminosity measurement. The largest systematic uncertainty of these analyses is 5% from the signal and background yield estimation for W $\rightarrow$ eν.

Table 1: Results for the $W \rightarrow e\nu$ cross section measurement

$N_{selected} - N_{bkgd}$	67954 $\pm$ 674
Tag&Probe ε_{total}	65.1 $\pm$ 0.5 %
Acceptance	52.3 $\pm$ 0.2 %
Int. Luminosity	10 pb^{-1}
$\sigma_W \times BR$(W $\rightarrow$ eν)	19.97 $\pm$ 0.25 nb
cross section used	19.78 nb

6 Conclusions

Analysis strategies for measuring the inclusive production cross-sections of the W and Z bosons have been formulated and tested for the early data-taking

Table 2: Results for the $\gamma^*/\mathrm{Z} \to \mathrm{e}^+\mathrm{e}^-$ cross section measurement

$N_{selected}$	3914 ± 63
N_{bkgd}	assumed 0.0
Tag&Probe ε_{total}	68.1 ± 0.6 %
Acceptance	32.39 ± 0.18 %
Int. Luminosity	10 pb^{-1}
$\sigma_{Z/\gamma^*} \times BR(Z/\gamma^* \to e^+e^-)$	1775 ± 34 pb
cross section used	1787 pb

period of CMS. These strategies must handle data before precise calibration and alignment can be carried out and so use robust selections and data-driven methods to extract efficiencies and background-corrected signal yields. Significant results can be obtained with only $10\,\mathrm{pb}^{-1}$ of data.

References

1. CMS Collaboration, Towards a Measurement of the Inclusive W $\to$ eν and $\gamma^*/\mathrm{Z} \to \mathrm{e}^+\mathrm{e}^-$ Cross Sections in pp Collisions at $\sqrt{s}$ =14 TeV, CMS PAS EWK-2007/001.

2. CMS Collaboration, Towards a Measurement of the Inclusive W $\to \mu\nu$ and $\mathrm{Z} \to \mu^+\mu^-$ Cross Sections in pp Collisions at $\sqrt{s}$ =14 TeV, CMS PAS EWK-2007/002

3. CERN, Standard Model Physics (and more) at the LHC, CERN-2000-004

4. LEP Electroweak Working Group, Precision Electroweak Measurements and Constraints on the Standard Model, CERN-PH-EP/2007-039

5. CMS Collaboration, Physics TDR Vol I. Detector Performance and Software, CERN/LHCC 2006-001.

6. CMS Collaboration, Data Acquisition & High-Level Trigger , TDR, CERN/LHCC 2002-26.

7. CMS Collaboration, Measuring Electron Efciencies at CMS with Early Data, CMS PAS EGM-2007/001